Biochimica et Biophysica Acta 1850 (2015) 1006–1016

Contents lists available at ScienceDirect

Biochimica et Biophysica Acta

journal homepage: www.elsevier.com/locate/bbagen

Review

# Electrostatic free energies in translational GTPases: Classic allostery and the rest☆

Thomas Simonson [a,*], Alexey Aleksandrov [a], Priyadarshi Satpati [a,b]

[a] Laboratoire de Biochimie (CNRS unit 7654), Department of Biology, Ecole Polytechnique, 91128 Palaiseau, France
[b] Department of Cell and Molecular Biology, University of Uppsala, Sweden

ARTICLE INFO

*Article history:*
Received 17 May 2014
Received in revised form 3 July 2014
Accepted 5 July 2014
Available online 15 July 2014

*Keywords:*
Molecular recognition
induced fit
molecular dynamics
continuum electrostatics
computational chemistry

ABSTRACT

GTPases typically switch between an inactive, OFF conformation and an active, ON conformation when a GDP ligand is replaced by GTP. Their ON/OFF populations and activity thus depend on the stabilities of four protein complexes, two apo-protein forms, and GTP/GDP in solution. A complete characterization is usually not possible experimentally and poses major challenges for simulations. We review the most important methodological challenges and we review thermodynamic data for two GTPases involved in translation of the genetic code: archaeal Initiation Factors 2 and 5B (aIF2, aIF5B). One main challenge is the multiplicity of states and conformations, including those of GTP/GDP in solution. Another is force field accuracy, especially for interactions of GTP/GDP with co-bound divalent $Mg^{2+}$ ions. The calculation of electrostatic free energies also poses specific challenges, and requires careful protocols. For aIF2, experiments and earlier simulations showed that it is a "classic" GTPase, with distinct ON/OFF conformations that prefer to bind GTP and GDP, respectively. For aIF5B, we recently proposed a non-classic mechanism, where the ON/OFF states differ only in the protonation state of Glu81 in the nucleotide binding pocket. This model is characterized here using free energy simulations. The methodological analysis should help future studies, while the aIF2, aIF5B examples illustrate the diversity of ATPase/GTPase mechanisms. This article is part of a Special Issue entitled Recent developments of molecular dynamics.



## 1. Introduction

GTPases and ATPases can hydrolyze GTP into GDP (or ATP into ADP), and they typically occupy different conformations depending on which nucleotide is bound [1,2]. This allows ligand-induced conformational switching, which underlies important biochemical processes, such as signaling and energy transduction [3–5]. Several GTPases/ATPases act as motors, like myosin and actin [6,7]. Others are kinases, including many important drug targets [8,9]. Still others act as molecular switches to help control processes like protein biosynthesis [10,11].

Conformational switching in these systems is triggered by the difference between GTP and GDP (or ATP and ADP), i.e., by a single phosphate group. This simple trigger can lead, however, to a great deal of complexity. Indeed, the protein typically has two distinct conformations or "states", which are respectively active, or ON and inactive, or OFF. Each state can bind either nucleotide, for a total of four complexes and four unbound molecules. The nucleotides themselves can bind one or more $Mg^{2+}$ ions. Usually, the ON protein can also bind one or more downstream, target molecules [10,11], which can be proteins or RNA. The complexity increases even further if we are interested in one or more inhibitors and/or several GTPases competing to bind the same inhibitor(s).

While experiments have given a wealth of information, computer simulations are an essential complementary tool [12]. They allow us to isolate individual conformational states, including complexes like ON:GDP or OFF:GTP that are weakly populated ("ON" refers to the protein in its ON state), and they can provide free energy values for each molecule and state. However, GTPases pose specific challenges, and a complete study is very much at the limit of today's simulation capabilities. We distinguish three sets of difficulties. The first is to account for the multiplicity of available states. This includes the protein ON and OFF states, but also many variations of these, corresponding to alternate protonation states or different numbers and positions of bound $Mg^{2+}$ ions, for example. For the unbound nucleotides, there are also a variety of structures and $Mg^{2+}$ coordination modes [13]. Accounting for all these structures and states can be viewed as a sampling problem, for which advanced, general methods are very much a current issue [14–17]. The second difficulty is to accurately model the molecular interactions. In particular, the nucleotide ligand usually coordinates a divalent $Mg^{2+}$ ion, which can polarize the electronic distribution of its environment, so that a quantum treatment or a sophisticated,

*Abbreviations:* ATP/GTP, adenosine/guanosine triphospate; aIF2/aIF5B, archaeal Initiation Factor 2/5B; IS/OS, Inner/Outer Sphere; MD, molecular dynamics; MDFE, molecular dynamics free energy; PBFE, Poisson–Boltzmann free energy

☆ This article is part of a Special Issue entitled Recent developments of molecular dynamics.

* Corresponding author. Tel.: +33 16933 4860.
*E-mail address:* thomas.simonson@polytechnique.fr (T. Simonson).

http://dx.doi.org/10.1016/j.bbagen.2014.07.006
0304-4165/

polarizable force field may be required [18,19]. The third set of difficulties has to do with electrostatic free energy calculations, and stems from the long-range nature of the Coulomb charge–charge interaction [20,21].

To represent this class of proteins, we will consider the archaeal Initiation Factors 2 and 5B, or aIF2 and aIF5B [22,23]. These are universally-conserved factors that play important roles in the translation of messenger RNA into protein. aIF2 is largely responsible for recruiting the first, initiator tRNA to the ribosome and positioning it correctly, in register with the start codon of the ribosome-bound messenger RNA [11]. It is thought to follow a classic allosteric activation mechanism, although experimental thermodynamic data is very sparse. Its ON and OFF structures are known; the main ON/OFF differences are localized in two conserved regions, called switch 1 and switch 2, within the GTP-binding $\gamma$ domain [24,22]. The relative stabilities of its different states were characterized by free energy simulations [25–27], showing that its GTP complex has a higher tendency to be ON while its GDP complex prefers to be OFF, favoring tRNA release and dissociation from the ribosome. aIF5B also assists initiator tRNA:ribosome binding and contributes essentially to ribosomal subunit joining [28–30]. Its structures and mechanism are not fully characterized, and several models have been proposed [23,28,31,32]. One of them does not involve any ON/OFF conformational changes.

In this paper, we review briefly our recent simulation work on aIF2 and aIF5B, as well as GTP and GDP in solution. We use aIF2 to show how a single phosphate group can trigger conformational switching. aIF2 also illustrates the thermodynamic cycles and the free energies that are needed to describe the main GTPase states. We use aIF5B to illustrate another, hypothetical, non-classical mechanism that departs from the usual GTPase picture but can nevertheless produce the required allosteric behavior. The model postulates that ON/OFF aIF5B have essentially the same conformation in the vicinity of the bound nucleotide, but differ by the protonation state of a single nucleotide-binding sidechain [23]. For this system, we present new free energy results concerning protonation states in the nucleotide binding pocket; these allow us to update and reformulate our earlier "Electrostatic" model. All these systems provide examples of the methodological difficulties mentioned above: existence of multiple states for the protein and nucleotides; force field accuracy, and long-range electrostatic interactions.

In the next section, we review the structure of GTP and GDP in solution, and the possibilities and limitations of different force fields. We then describe the simulation method we use to simulate both GTPases and compute free energies. We consider possible artifacts for the electrostatic free energies, which arise from the use of a periodic simulation model and the long-range of the Coulomb interaction. Next, we review briefly the mechanism of aIF2, in the context of a general thermodynamic framework for GTPases/ATPases. Our free energy simulations lead to a plausible picture, with a classical ON/OFF switching, driven by the additional GTP phosphate. Finally, we present new simulation results for aIF5B and use them to characterize a non-classical, Electrostatic model proposed recently for this protein's allosteric mechanism [23]. We conclude with a brief discussion. The detailed computational methods are given at the end.

## 2. NTP and NDP in solution

In the activation of a GTPase, the stability of both the bound and unbound nucleotides play an important role. For example, the interactions between the nucleotide's phosphate groups and any associated $Mg^{2+}$ ions will usually be different in the unbound and bound states, and between nucleotides. A requirement to evaluate nucleotide binding is thus to correctly identify the most important conformations of the unbound nucleotide, the cation, and its coordinating water molecules. Experimental and computational data were reviewed recently [13] and are summarized here for completeness. Most of the data are for ATP/ADP; GTP/GDP is expected to behave similarly. We refer to ATP and GTP as "NTP"; similarly for ADP/GDP.

NTP can explore a variety of conformations, including ones where the phosphates are extended away from the base (85% of PDB structures) or bent back towards the base (mostly complexes with 2 or 3 $Mg^{2+}$ per nucleotide) [33,34]. $Mg^{2+}$ can be coordinated by one, two, or three phosphates at a time. Of 285 PDB structures including NTP, most display $Mg^{2+}$ coordination of the $\beta$ and $\gamma$ phosphates but not $\alpha$. Each NDP/NTP phosphate can coordinate $Mg^{2+}$ in a mono- or bidentate manner (with one or two coordinating oxygens). Bi-dentate coordination is very rare in the PDB [25]. Ab initio methods predict that monodentate coordination is slightly more stable for the phosphate ions $H_2PO_4^-$ and $HPO_4^{2-}$ in solution; however the ab initio method gives poor agreement with the experimental $Mg^{2+}$:phosphate binding free energy [25].

The $Mg^{2+}$ ion can be coordinated directly ("Inner Sphere", or IS coordination) or through a bridging water molecule ("Outer Sphere", or OS) [35,36]. Recently, we compared the free energies for Outer Sphere $Mg^{2+}$ binding to GTP and GDP, and found them to be very similar [13]. The overall binding free energies are known to differ by about 2.1 kcal/mol [37]; together, these data imply [13] that the NTP:Mg complex is predominantly (at least 95%) Inner Sphere. The IS/OS populations for NDP are unknown. For $H_2PO_4$ and $HPO_4^{2-}$ in solution, ab initio methods predict that IS/OS are about equistable [25]. IS is predominant in PDB RNA structures (including the ribosome [38]), with some OS examples.

Experimental measurements of the binding free energies of $Mg^{2+}$ to ATP and ADP have been reviewed by Goldberg & Tewari [37,39], including several different experimental techniques, which have different sensitivities to IS/OS structures. The measured ATP/ADP free energy differences range from 1.5 to 2.4 kcal/mol, favoring ATP. The qualitative agreement between techniques means that the IS/OS sensitivities are not too different, or the OS subspecies is not important enough to affect the bound population significantly, or a combination of both.

Finally, we recall that with bound $Mg^{2+}$, the NTP/NDP phosphates are fully deprotonated most of the time, with an NTP $\gamma$ phosphate $pK_a$ of 4.7 and an NDP $\beta$ phosphate $pK_a$ of about 5.5 [40,41]. It remains to be seen whether these $pK_a$ values and protonation states are equally representative of IS and OS structures, or whether the proportion of protonated terminal phosphates is higher for OS complexes. In the absence of $Mg^{2+}$, the $\gamma$ phosphate $pK_a$ is about 7 [41]. Given the overall ATP:$Mg^{2+}$ binding free energy, $\Delta G_{bind} = -8.6$ kcal/mol [37,41,42] and the $\gamma$ phosphate $pK_a$'s with and without $Mg^{2+}$, $pK_1$ and $pK_2$, we may compute the ATP:$Mg^{2+}$ binding free energy $\Delta G_{bind}(GTP^-)$ of the deprotonated form separately:

$$\Delta G_{bind}(GTP^-) = \Delta G_{bind} + kTln\frac{1+e^{-\beta\Delta G_1}}{1+e^{-\beta\Delta G_0}}, \quad (1)$$

where $\beta = 1/kT$ is the inverse temperature; $\Delta G_1 = 1.35\ (pH - pK_1) = 3.1$ kcal/mol and $\Delta G_0 = 0$ are the protonation free energies at pH = 7 in the presence/absence of $Mg^{2+}$. This leads to $\Delta G_{bind}(GTP^-) = \Delta G_{bind} - 0.4$ kcal/mol $= -9.0$ kcal/mol. The 0.4 kcal/mol increment represents entropic stabilization of apo-GTP by its two equistable protonation states. $Mg^{2+}$ binding to protonated GTP is 3.1 kcal/mol less favorable.

Fixed charge force fields such as Charmm27 have been used to simulate NTP/NDP and many protein-NTP complexes in solution. With slight van der Waals parameter optimization [13], these models give realistic structures, including a realistic preference for GTP:Mg with $\beta + \gamma$ phosphate coordination. However, the $Mg^{2+}$ binding free energies and the GTP/GDP binding free energy difference are much harder to reproduce, and are overestimated by as much as 8–9 kcal/mol, presumably because there is no explicit polarizability. Similar errors are observed for the $Mg^{2+}$:$H_2PO_4^-$ and $Mg^{2+}$:$HPO_4^{2-}$

binding free energies [25]. In contrast, with the AMOEBA polarizable force field [43] (implemented in Tinker [44]) the $Mg^{2+}$:$H_2PO_4^-$ binding free energy is in much better qualitative agreement with experiment, with an error of just 2–3 kcal/mol (Simonson, Ohanessian, Clavaguera, unpublished data). The AMOEBA force field includes fixed charges and sometimes dipoles and quadrupoles on each atom, as well as polarizable dipoles. Evidently, with polarizable atoms, there is a much better balance between the $Mg^{2+}$:phosphate complexes and the separate partners. Slight force field parameter tuning could lead to even better agreement; details will be published elsewhere.

## 3. Electrostatic free energy simulations

To elucidate GTPase function, we need to compare the stabilities of GTP and GDP complexes, which is commonly done by alchemically transforming one into the other in a series of MD (or Monte Carlo) simulations [45,46]. This process modifies the net charge by $\pm 1$. We may also need to determine protonation free energies, which can also be done by alchemical insertion of a proton. Such charging free energy calculations involve specific difficulties, reviewed recently [21] and summarized here. We limit the discussion to the most common setup: a simulation box that is replicated through periodic boundary conditions (PBC). Long-range interactions are computed with Ewald summation (or a variant like Particle Mesh Ewald, PME) [47–50] or with a cutoff combined with a continuum reaction field (CRF) [51,52].

While experimental systems are finite, simulation models with PBC are infinite, which leads to three major artifacts [21]. (A) The simulation model fills all of space; it has no physical boundary, and so charge cannot be brought into the system from a distant, gas phase reference system, across a gas/liquid interface. The potential drop across such an interface is very large (over 10 kcal/mol/e for TIP3P water [53]); its effect is missing here. (B) The electrostatic potential at a particular location takes the form of an infinite sum of atomic or molecular contributions; unfortunately this sum is only semi-convergent [47,54], and so there are several possible results that are all mathematically correct [20,55,56]. For example, two commonly-used methods like PME and CRF can give potentials in liquid water that differ by over 10 kcal/mol [20,55–57]. (C) Finally, if we use PME with tinfoil boundary conditions, there is a third artifact. With tinfoil boundary conditions, the system, though infinite, is nevertheless assumed to be embedded in a surrounding conducting medium. As a result, whenever a charge is introduced, there is a uniform, neutralizing charge density that appears and maintains overall neutrality [47–50]. The neutralizing density is referred to as a "gellium" (or sometimes "jellium"). As a result, when we introduce a perturbing charge $q$, it experiences an effective electrostatic potential that is shifted, relative to the usual gas phase reference system. Specifically, the potential in the simulation box is shifted so that the box average is zero at all times [21,47–50]. This potential shift is system-dependent and directly affects electrostatic free energies.

Fortunately, all these artifacts can be handled with established protocols, as detailed below in the cases of aIF2, aIF5B. Briefly, the lack of a gas/liquid boundary (A) is not important as long as we compare molecules that are all in aqueous solution, like GTP/GDP bound to the protein or free in solution. In that case, we effectively move charges from one part of the solution to another, and there is no need to cross a gas/liquid boundary. The semi-convergence of the electrostatic potential (B) affects charging free energies, but in a simple way, and its effect cancels out for processes that conserve the total charge [21]. This is the case when we transform GTP into GDP in complex with the protein, while simultaneously changing GDP into GTP in solution. Finally, the potential shift imposed by PME with tinfoil boundary conditions (C) will cancel out when we compare binding to the ON/OFF states, or binding of GTP/GDP. It does not cancel out, however, when we compare GTP → GDP transformations in the protein and in solution, or when we compare sidechain protonation in the protein and in solution. We show below that with our simulation box sizes (≈80 Å), it can introduce a systematic error of about 1 kcal/mol for such comparisons. The same systematic error is present (though not always discussed) in other MDFE studies that compute charging free energies with PME; see Lin et al. for a recent review [21].

Efficiency is another important concern. Indeed, to obtain converged free energies, extensive sampling is needed. While this can be facilitated by specialized methods such as replica exchange [14–17], very long simulations are usually needed. Therefore, most of our simulations were done with the Charmm27 force field, which employs fixed atomic charges, modeling electronic polarization in an implicit way [58]. With this force field, we assume that the effect of electronic polarization by the divalent $Mg^{2+}$ will approximately cancel when the horizontal GTP → GDP legs of the cycle are subtracted. We refer to this assumption as the "additivity" hypothesis. Furthermore, we employ a multi-scale model (Fig. 1): protein regions close to the nucleotide are modeled in atomic detail, and distant regions are modeled as a simple dielectric medium [25,59,60]. With this model, MD simulations are performed for a spherically-truncated protein, solvated by a large cubic water box. In a separate stage, the free energy contribution of the truncated protein regions is obtained by solving the Poisson–Boltzmann equation numerically [25,59,60]. A variant of this general method is to include the distant dielectric medium directly in the MD simulation stage [61,62].

## 4. aIF2 as a classical GTPase

### 4.1. A general thermodynamic framework

To discuss GTPase activation and conformational switching, we use the thermodynamic cycle in Fig. 2. Vertical legs correspond to GTP or GDP binding, with the protein restricted to be in its ON or OFF state. The nucleotide preferences of each state, and the state preferences of each nucleotide, are characterized by the free energy differences

$$\Delta\Delta G_{ON} = \Delta G_{ON}(GTP) - \Delta G_{ON}(GDP) \tag{2}$$

$$\Delta\Delta G_{OFF} = \Delta G_{OFF}(GTP) - \Delta G_{OFF}(GDP) \tag{3}$$

$$\Delta\Delta G_{GNP} = \Delta G_{ON}(GNP) - \Delta G_{OFF}(GNP) \tag{4}$$

where $\Delta G_{ON}$(GNP) is the ON:GNP binding free energy and similarly for OFF. The system can be also characterized by the triple free energy difference:

$$\Delta\Delta\Delta G = \Delta\Delta G_{GTP} - \Delta\Delta G_{GDP} = \Delta\Delta G_{ON} - \Delta\Delta G_{OFF} \le 0 \tag{5}$$

$\Delta\Delta\Delta G$ is negative *by definition* of the ON/OFF states; a large magnitude indicates a large GTPase specificity. For example, if ON and OFF both have large preferences for their respective nucleotides, $\Delta\Delta G_{ON}$ is large and negative, $\Delta\Delta G_{OFF}$ is large and positive, and $\Delta\Delta\Delta G$ is large and negative. Notice however that $\Delta\Delta G_{ON}$ and $\Delta\Delta G_{OFF}$ can have the same sign; for example, both states may prefer to bind GTP (as long as $\Delta\Delta\Delta G \le 0$). Such GTPases are considered "non-classical" [63].

We can express the overall binding free energy difference $\Delta\Delta G_{bind} = \Delta G_{bind}(GTP) - \Delta G_{bind}(GDP)$ as a function of the values in Fig. 2. Denoting $G$(ON:GNP), $G$(OFF:GNP) the free energies of the ON/OFF complexes, we have [45]:

$$e^{-\beta\Delta G_{bind}(GNP)} = \frac{e^{-\beta G(ON:GNP)} + e^{-\beta G(OFF:GNP)}}{e^{-\beta G(ON)} + e^{-\beta G(OFF)}}\; e^{\beta G(GNP)} \tag{6}$$

$$e^{-\beta\Delta\Delta G_{bind}} = e^{-\beta\Delta\Delta G_{ON}}\,\frac{e^{-\beta x(GTP)}+1}{e^{-\beta x(GDP)}+1} = e^{-\beta\Delta\Delta G_{OFF}}\,\frac{e^{\beta x(GTP)}+1}{e^{\beta x(GDP)}+1} \tag{7}$$

where $x$(GNP) = $G$(ON:GNP) − $G$(OFF:GNP). Noticing that $x$(GTP)

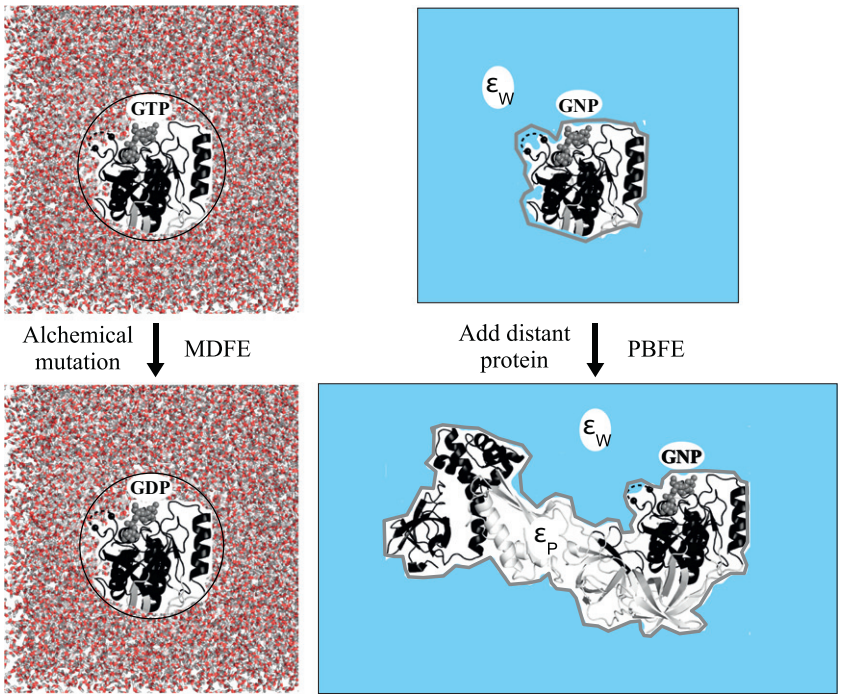


**Fig. 1.** Multi-scale approach for electrostatic free energies. Atoms in a spherical region are described in detail, solvated by a large volume of explicit water (left). The free energy contribution of more distant protein is computed separately, using a Poisson–Boltzmann free energy method that treats the protein and surrounding solvent as two dielectric media (right).

$-x(\mathrm{GDP}) = \Delta\Delta\Delta G \le 0$, we see that $\Delta\Delta G_{\mathrm{bind}}$ is intermediate between the ON and OFF values:

$$\Delta\Delta G_{\mathrm{ON}} \le \Delta\Delta G_{\mathrm{bind}} \le \Delta\Delta G_{\mathrm{OFF}} \quad (8)$$

Eq. (1), used above for GTP:$Mg^{2+}$ binding, was a special case of Eq. (7).

Eqs. (2–8) are completely general. The ON/OFF populations depend on the relative stabilities of four complexes: ON:GTP, ON:GDP, OFF:GTP and OFF:GDP, as well as apo-ON, apo-OFF and unbound GTP/GDP. For aIF2, while the overall GDP binding constant (0.5 μM) is known for one organism (*Pyrococcus furiosus*), none of the four, individual binding constants (ON:GTP, ON:GDP, OFF:GTP, OFF:GDP) are known experimentally, nor is the apo-ON/OFF free energy difference. The conformational changes that define the ON/OFF states are mainly localized in two conserved of 20 amino acids each, called switch 1 and switch 2. GTP and GDP bind in a pocket at the surface of the γ subunit, making contact with both switches. In the ON and OFF states, a $Mg^{2+}$ ion coordinates the phosphate groups—the β and γ groups of GTP and the β group of GDP. X-ray structures have been determined for apo-aIF2 and for complexes with GTP and GDP. Interestingly, a structure of aIF2 in its OFF state was obtained with bound GTP [24]. The structure of the ON:GDP complex is unknown (and probably weakly-populated).

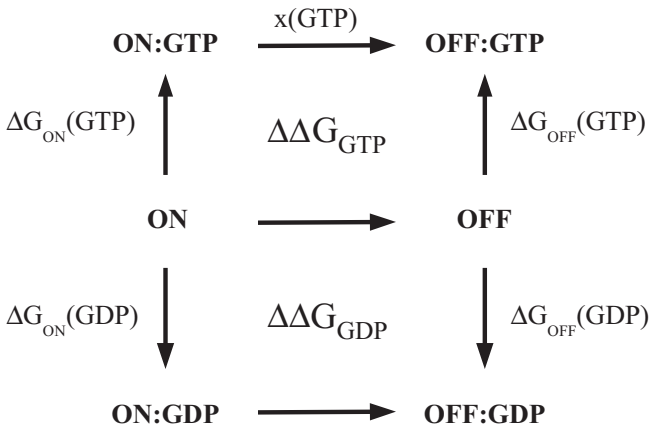


**Fig. 2.** Thermodynamic cycle for GTPase analysis. Vertical legs represent nucleotide binding to the ON (left) or OFF (right) protein. Free energies for some of the legs are labeled.

### 4.2. The free energy simulation approach

Recently, we reported a free energy simulation study of aIF2 [25–27]. To compute GTP/GDP binding free energy differences, we alchemically and reversibly transformed GTP into GDP over the course of long molecular dynamics simulations [64–68]. We refer to this as the MD Free Energy method, or MDFE [65]. By performing the transformation both for the ligand alone in solution and bound to the ON or OFF protein, we obtained the GTP/GDP binding free energy differences [69]. Notice that in the limit of very long simulations, the protein could spontaneously change from the ON to the OFF state or vice versa, so that specific restraints could be needed to impose one or the other. In our work, the outer part of the protein model is harmonically restrained (see Computational methods), and the ON/OFF states did not interchange.

Replacing GTP by GDP removes one $Mg^{2+}$:phosphate interaction. To test the importance of electronic polarizability, we repeated here our earlier calculations [25], which compared the Charmm27 fixed charge force field and the polarizable, AMOEBA force field (extended to include GTP). We computed a quantity δG that approximates the

**Table 1**
Force field sensitivity of the δG free energy estimator in aIF2.

| | AMOEBA | Charmm27 |
|---|---|---|
| ON/solution difference | 4.3 (2.1) | 7.2 (1.4) |
| OFF/solution difference | 2.2 (3.0) | 2.1 (1.5) |
| ON/OFF difference | 2.1 (2.0) | 5.1 (1.2) |

In kcal/mol. Values in parentheses are the uncertainty, estimated as the half difference between the 1st and 2nd halves of each ensemble of structures.

free energy to change GTP into GDP; for details, see Computational methods and the earlier article [25]. Despite the errors observed for $Mg^{2+}$:phosphate binding with the Charmm27 force field [25], we observe a substantial cancelation of errors when we compare the free energy change $\delta G$ in the protein to that in solution, or when we compare the protein's ON and OFF states. Results are given in Table 1, based on MD simulations of 4–6 ns for the four protein states and 3 ns for the nucleotides in solution. The average Charmm/AMOEBA difference is 2 kcal/mol, around the statistical uncertainty. The largest discrepancy was that between the ON/OFF differences, 3.0 kcal/mol. Earlier results with shorter MD simulations (2 ns) gave comparable differences [25]. We also compared the ON/OFF binding free energy differences for GTP and GDP using a Poisson–Boltzmann free energy method (or PBFE) that explicitly includes the electronic polarizability of the solutes (through a dielectric constant greater than 1). We obtained good agreement with the MDFE results (obtained with the fixed-charge, Charmm27 force field), within 1–2 kcal/mol. Similar cancelation of errors was seen when comparing ATP/ADP binding to different ATP synthase structures [70,71]. We conclude that the "additivity" hypothesis is verified at least qualitatively, and the effect of electronic polarization by the divalent $Mg^{2+}$ will approximately cancel when the horizontal legs of our thermodynamic cycle (Fig. 2) are subtracted.

Another possible concern is the structural model around the $Mg^{2+}$ cation. In the ON:GTP X-ray structure, the 3 Å X-ray resolution led to an incorrect $Mg^{2+}$ position [72], which was corrected spontaneously during the MD simulations by a shift of about 1 Å [26]. When the protein was prepared for the MD simulations, slightly different protocols also led to some differences in the precise water positions near the $Mg^{2+}$ and nucleotide, some of which persisted over the length of the simulations (tens of nanoseconds). The main free energy results were not sensitive to these differences, but the detailed predictions vary somewhat between models [26].

Finally, we consider the potential issues (A–C) mentioned above for electrostatic free energy calculations. (A) Since we perform GTP → GDP transformations in solution and in complex with the protein, we effectively move charge from one place to another within aqueous solvent, and the lack of a physical gas/liquid boundary in the simulation model is not an issue. (B) Although the electrostatic potential is only semi-convergent, we showed earlier [21] that for processes that conserve the total charge, this has no effect on the free energy change. Taking the two transformations together, GTP → GDP in solution and GDP → GTP in the protein, the total charge is conserved, and so the free energy change is uniquely defined. (C) We use PME with tinfoil boundary conditions; therefore, the charges introduced by our alchemical GTP → GDP transformation (or protonation/deprotonation transformations, below) experience a shifted potential, whose average over the simulation box is constrained to be zero at all times. The magnitude of this shift depends on the solute structure, its net charge, and the amount of solvent in the simulation box [21]. It is different for the GTP:protein complex and for GTP in solution. In the limit of a very large box, both shifts (in protein, in solution) converge to a constant value, which only depends on the solvent. But for a finite box size, the two shifts are different, and this affects our MDFE estimates of $\Delta\Delta G_{ON}$ and $\Delta\Delta G_{OFF}$. It will also affect the protonation free energies computed for His80, Glu81 in aIF5B, below.

Fortunately, with the box sizes used here, we are not too far from the large box limit, and the potential shift cancels to within about 1 kcal/mol when we compare GTP → GDP in solution and in aIF2. Indeed, the volume fraction of protein in the 80 Å simulation box is about 15%. The potential difference between the protein and solvent regions may be roughly estimated at around 240 mV [21]. This implies that the potential shift, compared to an infinitely large box, is about $0.15 \times 240$ mV ≡ 0.8 kcal/mol. While this error is not negligible, it is smaller than the statistical uncertainty for $\Delta\Delta G_{ON}$ and $\Delta\Delta G_{OFF}$, and does not alter our main conclusions.

#### 4.2.1. The driving forces for GTP/GDP-aIF2 binding

The simulations provide a quantitative estimate of the selectivity difference between the ON and OFF states. We found that the GTP/GDP binding free energy difference is small in the ON state, about −1 kcal/mol in favor of GTP, and larger in the OFF state, about +4 kcal/mol in favor of GDP. The signs are consistent with the experimental preferences for downstream tRNA binding [22] and the magnitudes seem sensible. Using a simpler, continuum electrostatic free energy method (PBFE), we decomposed the free energy differences further and characterized the binding preferences in terms of a few simple physical effects: ligand desolvation, direct protein:ligand interactions, and their shielding by solvent. The four protein:nucleotide complexes are schematized in Fig. 3.

There is a large free energy cost to (partially) desolvate either nucleotide by moving it into its binding site, along with its co-bound $Mg^{2+}$ ion. The penalty is larger for GTP:$Mg^{2+}$ (−2 charge) and for the ON state, which has a less open binding pocket, with fewer nearby waters. The differences were estimated with a PBFE dielectric continuum model using a solute dielectric constant of 4 [26]. The OFF GTP/GDP difference is 2.4 kcal/mol, fairly close to the overall GTP/GDP binding free energy difference of 4 kcal/mol. Indeed, the OFF-bound GTP γ-phosphate is still extensively solvated, coordinated by six waters, compared to nine for GTP in solution. The $Mg^{2+}$ coordination spheres in the GTP/GDP:OFF complexes are very similar: with GTP, $Mg^{2+}$ coordinates the β and γ phosphates and four waters; with GDP, a water replaces the γ phosphate in the coordination sphere. Nucleotide interactions with the OFF protein are quite similar for GTP and GDP, with large binding free energy contributions from Lys22 and Asp93, and an additional GDP interaction with the Asp19 backbone.

For the ON state, the situation is more complex. The GTP/GDP desolvation difference is very large, about 22 kcal/mol. Indeed, the ON binding pocket is much "dryer" than the OFF pocket, and the GTP γ-phosphate is now coordinated by just three waters. This desolvation penalty must be completely offset by favorable GTP:ON interactions, since the overall GTP/GDP binding free energy difference is just −1 kcal/mol (pro-GTP). A PBFE analysis identified several large ON:GTP interactions [26], especially Lys22 and to a lesser extent Asp22, which offset about 2/3 of the GTP/GDP desolvation difference. The rest of the binding free energy difference must arise from a larger set of much smaller contributions. The direct free energy contributions of the two switches are very small.

Finally, we studied complexes of aIF2 with the product of GTP hydrolysis: GDP plus inorganic phosphate Pi, and compared several possible pathways between this state and the final, OFF:GDP state [27]. The simulations suggest that a crystal structure that has both ON and OFF features [73] could be an intermediate on this pathway.

## 5. A non-classic, electrostatic model for aIF5B

Our second GTPase example is the archaeal Initiation Factor 5B, aIF5B. Crystal structures of aIF5B with GTP and GDP are very similar near the nucleotide [28], but differ in the orientation of a distant domain. This has led to contradictory mechanistic models. One postulates [28] that the two complexes are ON and OFF respectively, and the GTP/GDP exchange drives the distant domain motion. Another postulates [31] that both structures are OFF, and the ON structure is unknown. We recently proposed a third, "Electrostatic" model [23]. With this model, the ON/OFF states have the same conformation, and differ by a single proton that binds to nearby Glu81 when GTP is bound; see Fig. 4. No distant, allosteric conformational change occurs because of GTP binding (although changes may occur upon downstream ribosome binding). The model assumes that the stronger ribosome binding by the aIF5B:GTP complex, relative to aIF5B:GDP, can be accounted for by the different charge distributions in the two complexes, without the need for switch rearrangements or distant domain motions. The ribosome binding increase could be provided, for example, by direct contacts

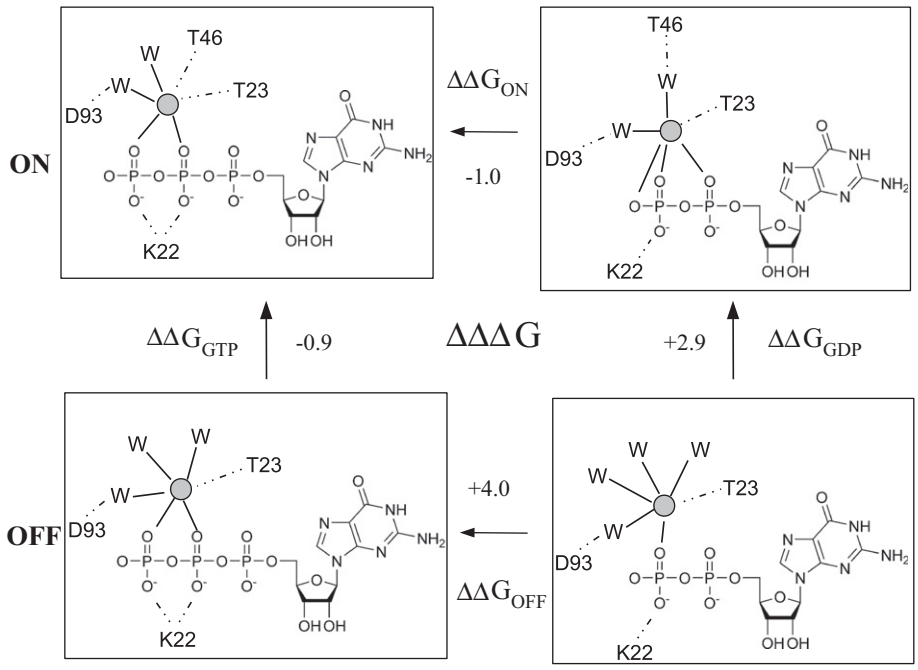


**Fig. 3.** Schematic view of the aIF2:nucleotide complexes in the form of a thermodynamic cycle. Free energies from MDFE (horizontal legs) and PBFE (vertical legs) are indicated. Water and nucleotide coordination of the $Mg^{2+}$ ion (gray disk) is shown by solid lines; other hydrogen bond interactions are shown as dashed lines.
Reproduced from Proteins, 80:1264; copyright Wiley, Inc.

between Glu81, GTP, and the ribosome, similar to contacts seen in the homologous EF-Tu:ribosome crystal complex [74].

To analyze the Electrostatic model, we use the thermodynamic cycle in Fig. 2. Its seven legs define seven free energy differences. These are connected through two closure relations (the sum over each closed cycle is zero). For the vertical legs, since we always consider GTP/GDP differences, one of the four values can be arbitrarily set to zero without loss of generality. The GTP/GDP binding free energy difference for the ON state was estimated earlier with a PBFE continuum dielectric method [23]: $\Delta\Delta G_{ON} = -0.8$ kcal/mol. The ON → OFF free energy difference (middle leg) corresponds to Glu81 deprotonation in the apo-protein, and was estimated [23] to be −4.0 kcal/mol using the PropKa program. PropKa implements an accurate semi-empirical model for acid/base reactions; its typical error is about 1 kcal/mol [75,76]. Finally, two more free energy differences were computed in this work, corresponding to Glu81 protonation in the presence of bound GTP or GDP. These values were obtained with the MDFE method [46,77], using long MD simulations (see Computation methods). With these 7 free energies in hand, we can compute several quantities that characterize the protein's state and nucleotide preferences, as well as the overall nucleotide preference. The results differ somewhat from our earlier analysis [23], which used different information, including the experimental GTP/GDP binding free energy difference from a bacterial orthologue. Before presenting this analysis, we describe the free energy simulation results and the protonation states in the nucleotide binding pocket.

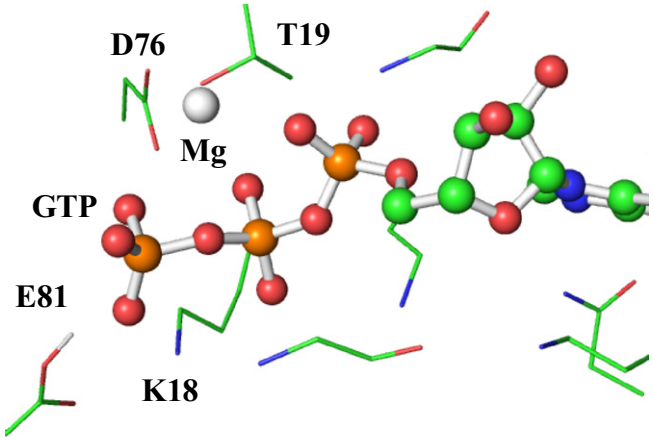


**Fig. 4.** Closeup of the binding pocket of aIF5B:GTP. Hydrogens are omitted, except for protonated Glu81. The $Mg^{2+}$ position differs from the crystal structure but agrees with several homologous proteins.

### 5.1. Protonation free energies in aIF5B

We considered two sidechains in the nucleotide binding pocket that can bind a proton: His80 and Glu81, and we also compared two GTP protonation states. Glu81 is the group that defines the ON/OFF states of aIF5B in our Electrostatic model. To compute the protonation free energy of either group, we use an established method that deprotonates the sidechain in the protein and a sidechain analog in solution [77,78]. By comparing the two reactions, we actually compute the shift in the deprotonation free energy due to the protein environment. By adding back the experimental free energy to deprotonate the analog in solution, we can deduce the sidechain deprotonation free energy in the protein at a given pH.

In the crystal complex with GTP, Glu81 forms a hydrogen bond with the GTP γ phosphate (Fig. 4). This implies that in the crystal, there is a proton either on Glu81 or the GTP γ phosphate. Here, we compare the free energies of three possible arrangements: (protonated Glu81 + deprotonated GTP), (deprotonated Glu81 + protonated GTP), and (deprotonated Glu81 + deprotonated GTP). For His80, we compared the sidechain in its two singly-protonated states (on ND1 or NE2) and its doubly-protonated state (on ND1 and NE2). When the bound nucleotide is GDP, we assume it is always fully-deprotonated (for a net charge of −3). We mention here that the GTP crystal complex [28] has an incorrect $Mg^{2+}$ position, on the wrong side of GTP compared to several homologous structures. The position was spontaneously corrected during MD (similar to aIF2, above).

We begin by considering the systematic error introduced by PME with tinfoil boundary conditions: the mean box potential is shifted so

as to ensure a box average of zero at all times. This shift differs for the protein and the sidechain analog in solution, because the two simulation boxes have very different solvent fractions. We estimated above the potential shift due to the protein volume in an 80 Å box (close to the value used here): the potential is shifted by about 0.8 kcal/mol/e, compared to a very large box. This estimate was based on the protein volume fraction and a rough, consensus estimate of 240 mV for the potential drop between the protein and solvent regions [21]. It is supported further by a comparison of the electrostatic potential in aIF5B using MD simulations with an 81 Å or 68 Å box. With the larger box, the mean potential on the $C_\alpha$'s is increased by about 0.7 kcal/mol. An increase is expected (larger solvent fraction in the box). Its magnitude agrees with the estimate we obtain assuming the consensus 240 mV potential drop. Indeed, the solvent fraction increases by about 0.10 with the larger box, for an increase of the potential shift by $0.10 \times 240$ mV ≡ 0.5 kcal/mol. Overall, the finite box size introduces a systematic error of about 1 kcal/mol for the Glu81 and His80 protonation free energies. A more precise error estimate could be obtained by performing Poisson–Boltzmann calculations of the electrostatic potential [21]. However, we consider the present error estimate acceptable for our purposes.

When the group of interest is the γ phosphate of unbound GTP, a specific difficulty arises: the $Mg^{2+}$ coordination changes when a proton binds. The corresponding free energy change is then unreliable, because the Charmm27 force field cannot accurately compare different $Mg^{2+}$ coordination free energies [13]. Therefore, we used a simpler free energy method for GTP protonation: structures of the aIF5B:GTP complex are extracted from an MD simulation and the free energy is computed from a Poisson–Boltzmann continuum electrostatic model. The calculation is done for either GTP protonation state. The same GTP conformations are also used to compute the free energies of unbound GTP (in either protonation state), so that no $Mg^{2+}$ rearrangement can occur. The free energies are combined to obtain the GTP protonation free energy. This method is referred to as the PB/LRA method [78–82], where LRA stands for Linear Response Approximation. It has given accurate results for several test systems [80–82], including Glu81 protonation in the aIF5B:GDP complex (see below). With PB/LRA, the electrostatic potential is computed by solving the PB equation, so the systematic shift due to tinfoil boundary conditions does not play any role.

The relative free energies of all the possible states are listed in Table 2. Uncertainties are moderate, thanks to the 50 ns run lengths. With bound GDP, the most stable state has Glu81 ionized and His80 either singly- or doubly-protonated (the two His variants differ by just 0.2 kcal/mol). With bound GTP, the most stable state has protonated Glu81 and deprotonated GTP; His80 has a moderate preference to be doubly-protonated. The free energy to transfer the proton from Glu81 to GTP is rather high, 4.7 kcal/mol (using PB/LRA and a solute dielectric constant of two, and taking into account the $pK_a$ difference of 0.4 between the two groups). Thus, this state is weakly-populated and can be neglected. The free energy to ionize Glu81, while forcing GTP to remain deprotonated, is 5.3 kcal/mol (this and all the other protonation free energies are given for a pH of 7). The free energy to protonate a Glu sidechain analog in solution at this pH is about 3.6 kcal/mol (since the $pK_a$ is 4.3) [83]. Thus, the $pK_a$ of Glu81 when GDP is bound is downshifted by about 1.2 units compared to Glu in solution. This small $pK_a$ shift is within the uncertainty of the MDFE calculations. It is close to our earlier estimate, a 0.7 downshift [23], using the PB/LRA, continuum electrostatic free energy method.

**Table 2**
Free energies (kcal/mol) for different protonation states in aIF5B.

| Charge state | | Free energy | | GTP |
|---|---|---|---|---|
| H80[a] | E81 | GDP | GTP | Charge |
| (+) | 0 | 5.5 (1.2) | −1.6 (0.8) | −4 |
| NE2 | 0 | 4.7 (1.1) | 0.0[b] | −4 |
| ND1 | 0 | 4.6 (1.0) | −0.1 (0.5) | −4 |
| (+) | −1 | −0.2 (0.5) | 4.2 (1.4) | −4 |
| NE2 | −1 | 0.0[b] | 7.9 (1.2) | −4 |
| ND1 | −1 | 2.1 (0.8) | 7.6 (1.2) | −4 |
| ND1 | −1 | – | [c]4.6 (0.1) | −3 |

[a]For His80, we indicate the single protonated nitrogen or "+" if both are protonated. [b]One state is taken arbitrarily as the free energy origin. [c]Obtained using the PB/LRA method.

When Glu81 and GTP are both deprotonated, the situation is complicated, because one of 7 potassium counterions moves from the solution region of the simulation box to bind between the two groups. Since the box has an 81 Å edge length, the potassium concentration is 22 mM, not too far from the physiological value. If the solution concentration was increased (decreased) by 10, the free energy to remove a potassium from the bulk would decrease (increase) by about 1.35 kcal/mol, and the Glu81 deprotonation would decrease (increase) by the same amount. Thus, we may assume our free energy to deprotonate Glu81 (keeping GTP deprotonated) is valid, within about ±1.35 kcal/mol, as long as the concentration of small monovalent cations is less than the physiological ionic strength of about 150 mM. This uncertainty does not change the main observation: the GDP complex prefers to have Glu81 ionized ("OFF"); the GTP complex prefers Glu81 to be protonated ("ON"). In the next section, we put these free energies into the context of our Electrostatic model for aIF5B.

### 5.2. The Electrostatic model

We start from the general thermodynamic cycle in Fig. 2 [23,63]. The nucleotide preferences of each state are characterized by the free energy differences $\Delta\Delta G_{ON}$, $\Delta\Delta G_{OFF}$; the state preferences of each nucleotide are characterized by $\Delta\Delta G_{GNP}$, where GNP is GTP or GDP. The various free energies are related by the general Eqs. (2–8).

We now specialize to our Electrostatic model, postulating that ON/OFF only differs in the Glu81 protonation state: protonated is ON (preferred by GTP) and deprotonated is OFF (preferred by GDP). In that case, $x$(GNP) is the free energy to deprotonate Glu81 when the bound nucleotide is GNP, computed here using alchemical MDFE simulations [46,77]. $\Delta\Delta G_{ON} = -0.8$ kcal/mol was estimated earlier using a simpler continuum dielectric free energy method [23]. In our original analysis [23], $x$(GTP) was the unknown quantity, while $\Delta\Delta G_{bind}$ was approximated by the experimental value for a bacterial orthologue, 1 kcal/mol [31]. This allowed $x$(GTP) to be predicted (taking into account the uncertainties for $\Delta\Delta G_{ON}$, $\Delta\Delta G_{bind}$, and $x$(GDP)). The predicted value was −0.4 kcal/mol, meaning that the Glu81 $pK_a$ was only weakly upshifted by the GTP ligand. In fact, the more rigorous MDFE simulations above gave a much larger value: $x$(GTP) = +5.8 kcal/mol (at pH 7), meaning that the Glu81 $pK_a$ is strongly upshifted, and Glu81 deprotonation is very unfavorable with bound GTP.

The larger $x$(GTP) value is still compatible with our Electrostatic model. It can be reconciled with the earlier free energies through minor adjustments to the free energy values drawn from the simulations and experiments, within their uncertainties. To see this, we use the simulation results for $x$(GTP), $x$(GDP), and $\Delta\Delta G_{ON}$ to predict $\Delta\Delta G_{bind}$, as follows. We assume an uncertainty of ±2 kcal/mol for each simulation free energy, and for each one, we consider all the values within this range, in steps of 0.5 kcal/mol. For $x$(GTP), for example, the possible values are then 3.8, 4.3, 4.8, …, 7.8; similarly for $x$(GDP) and $\Delta\Delta G_{ON}$. There are about 700 such combinations, which we denote $\mathbf{X}$ = ($x$(GTP), $x$(GDP), $\Delta\Delta G_{ON}$). For each combination, we solve Eq. (7) to obtain $\Delta\Delta G_{bind}(\mathbf{X})$. The average value is $\langle\Delta\Delta G_{bind}\rangle_{\mathbf{X}} = 4.5 \pm 1.8$ kcal/mol, somewhat larger than the bacterial orthologue (1 kcal/mol). However, within the range of simulation free energy values, {**X**}, there is a subset "small" that gives back almost the same $\Delta\Delta G_{bind}$ as before [23]. Indeed, if we retain only the free energy combinations **X** that lead to a solution $\Delta\Delta G_{bind}(\mathbf{X})$ of 2 kcal/mol or less, we obtain $\langle\Delta\Delta G_{bind}\rangle_{small} = 1.6$ kcal/mol. The various free energy values, averaged over the full set {**X**} or the "small" subset are given in Table 3. Table 3 also recalls the values used or predicted in

**Table 3**
Electrostatic model for aIF5B: free energy values (kcal/mol).

| | Overall | Small | Earlier | | | |
|---|---|---|---|---|---|---|
| | Averages[a] | Subset[a] | Analysis[b] | IF2[c] | aIF2[d] | Neoclassical[e] |
| $G$(ON)–$G$(OFF) | −4.0 | −4.0 | −3.5 (0.7) | – | – | – |
| $\Delta\Delta G_{bind}$ | 4.5 (1.8) | 1.6 | 1.6 (0.5) | 1.0 | – | ≈2.0 |
| $x$(GTP) | 5.8 (2.0) | 5.6 | −0.4 (1.0) | – | – | ≈1.2 |
| $\Delta\Delta G_{GTP}$ | | −9.6 | −3.1 (1.0) | −3.4 | ≈−0.7 | – |
| $\Delta\Delta G_{GDP}$ | | −0.1 | 0.4 (0.7) | −1.2 | ≈+3.1 | – |
| $\Delta\Delta\Delta G$ | −11.1 | −9.5 | −3.4 (1.0) | −2.2 | −5.0 | ≤−2.5 |
| $\Delta\Delta G_{ON}$ | −0.8 (2.0) | −2.3 | −1.3 (0.7) | −0.1 (1.1) | −1.0 | ≤0.7 |
| $\Delta\Delta G_{OFF}$ | | 7.2 | 2.1(0.7) | 2.1 (1.1) | 4.0 | 3.2 |

[a]Values from this work, averaged over the full range of simulation free energy values {**X**} or the "small" subset; see main text. [b]Results from our earlier analysis [23], which used the experimental IF2 value for $\Delta\Delta G_{bind}$ and treated $x$(GTP) as an unknown. Uncertainty in parentheses. [c]Experimental results for the bacterial orthologue IF2 [32]. [d]Simulation results for the homologue aIF2, obtained earlier [26]. [e]Neo-classical model of aIF5B proposed by Hauryliuk et al. [31].

our earlier analysis [23]. The values that are significantly different are the ones that are closely linked to $x$(GTP), like $\Delta\Delta G_{OFF}$ (Fig. 2). Because of the simulation uncertainties (the range of **X**), the model does not allow a precise prediction for $\Delta\Delta G_{bind}$, but only a plausible range, 0–5 kcal/mol; the positive sign means an overall preference for GDP binding. The bacterial orthologue value (1 kcal/mol) is within this range, but the archaeal $\Delta\Delta G_{bind}$ may be somewhat larger.

## 6. Concluding discussion

The multiple conformations and binding partners of GTPases/ATPases usually prevent a complete experimental characterization, making them a prime target for simulations. Many aspects can be studied with standard fixed charge force fields and MD, including structure, dynamics, inhibitor binding and selectivity. However, the relative GTP/GDP binding free energies are sensitive to the strength of $Mg^{2+}$-phosphate interactions, which are not accurately described by fixed charge force fields [13,25]. High level quantum-mechanical (QM) and mixed QM/molecular mechanics methods can be used in principle, but are still much too expensive for thorough conformational sampling and accurate free energy calculations, which require either tens to hundreds of nanoseconds of MD, specialized sampling methods [14–17], or both. Also, while the errors are smaller for $Mg^{2+}$-phosphate binding with QM than with simple force fields, they remain substantial [25]. Polarizable force fields are expected to be a tool of choice; however, their testing and validation for complex proteins and nucleotides are still limited [43,84,85].

Here, we described a strategy based on an additivity hypothesis for the $Mg^{2+}$-phosphate interactions, which should be qualitatively valid [25,26]. Using this hypothesis, we have studied the nucleotide preferences of ON and OFF aIF2, using the Charmm27 force field and alchemical free energy simulations (MDFE). Free energy simulations involve several other challenges, especially for processes that introduce new charges, like the GTP → GDP alchemical transformation [21]. For the processes considered here, the most important artifact comes from the tinfoil boundary conditions used with PME, which impose a particular choice for the origin of the electrostatic potential. Since this choice is system-specific, it does not cancel out of our thermodynamic cycles. Despite rather large (80 Å) simulation box sizes, it introduces a systematic error that can be as large as 1 kcal/mol. Another issue is efficiency, and so we have introduced a multi-scale free energy strategy, with a continuum model for protein regions far from the nucleotide [60].

To analyze the GTPase mechanism, we use a general thermodynamic framework, introduced earlier [23,63] and summarized above (Eqs. (2–8)). As examples, we considered two translational GTPases. We showed that aIF2 behaves as a "classical" GTPase, consistent with the (very sparse) available experimental information. The simulations provided important insights into the sources of nucleotide specificity and ON/OFF conformational selection, with the help of a PBFE free energy component analysis. A more detailed testing of our simulations is not possible for now, since experimental thermodynamic data like the overall aIF2:GTP binding constant is lacking.

For aIF5B, we proposed a distinctly non-classical model, where the ON/OFF states have the same conformation but differ through protonation of Glu81, next to the bound nucleotide. We used free energy simulations to compute protonation free energies and characterize the model in some detail. Although the model remains hypothetical, it shows that an alternate GTPases mechanism is thermodynamically possible, and extends the classical framework normally used to analyze these proteins.

Overall, while this field poses major challenges to simulations, and will benefit substantially from the ongoing development of polarizable force fields, there are already many problems that can be studied and important insights to be obtained. The present review should help identify the main hurdles and approximations and facilitate future studies.

## 7. Computational methods

### 7.1. Structural models of aIF5B and MD setup

The crystal structures of the initiation factor aIF5B with bound GTP or GDP were taken from the PDB, entries 1G7T and 1G7S. The simulations included protein residues within a 30 Å sphere, centered on the nucleotide binding site. During MD, protein atoms between 25 and 30 Å from the center were harmonically restrained to their positions in the crystal structure (after a slight energy minimization). In addition to crystal waters, an 81 Å cubic box of water was overlaid, and waters overlapping the protein were removed. Periodic boundary conditions were assumed; i.e., the entire box was replicated periodically in all directions. Long range electrostatic interactions were computed by the particle mesh Ewald method (PME) with tinfoil boundary conditions [50], and the appropriate number of potassium counterions (6–7) were included to make the system electrically neutral. MD simulations were done at constant room temperature and pressure, after 200 ps of thermalization. The CHARMM27 force field was used for the protein [58,86] and the TIP3P model for water [87]. Protonation states of histidines other then His80 were assigned to be neutral, based on visual inspection. Calculations were done with the Charmm and NAMD programs [88,89].

### 7.2. Alchemical free energy simulations for aIF5B protonation

Alchemical MD free energy calculations (MDFE) [45,46,65,90] were done to compute free energy differences between protonation states of His80 and Glu81, with the methodology described earlier [77]. The method reversibly transforms a sidechain from one protonation state into another by gradually changing selected atomic charges. The charges are scaled, respectively, by 1-λ and λ, where λ is a weight, or "coupling parameter" that varies gradually from zero to one. The free energy derivative with respect to λ has the form $\partial G/\partial\lambda = \langle \partial U/\partial\lambda \rangle_\lambda$, where U is the energy function and the brackets indicate an average over an MD simulation performed with a particular value of λ. The derivative is integrated numerically to obtain $\Delta G$, using trapezoidal integration. Simulations corresponded to λ values of 0, 0.25, 0.5, 0.75, and 1.0. The procedure is applied to the protein:ligand complex and to a sidechain analog in solution. The analog included the His or Glu sidechain and its backbone, with neutral N-acetyl and N-methylamide blocking groups [77]. Subtracting the two free energies gives $\Delta\Delta G$, which measures the $pK_a$ shift of the sidechain relative to the analog. A complete MDFE run corresponded to 5 "windows" and 25 ns of simulation. For each transformation, we did a forward and a backward run, totaling 50 ns. The uncertainty was calculated as the standard deviation of the values obtained subdividing each window into five 1 ns segments.

### 7.3. PB/LRA free energy simulations for GTP protonation

For the protonation free energy of the GTP γ phosphate, in the aIF5B complex and alone in solution, we used a simpler, "Poisson–Boltzmann Linear Response Approximation", or PB/LRA [78–81]. Protonation of the phosphate group was modeled by changing selected atomic charges. The corresponding free energy change was computed both in the protein complex and for the ligand alone in solution, using conformations taken from a 5 ns aIF5B:GTP MD simulation with either (protonated GTP + ionized Glu81) or (deprotonated GTP + protonated Glu81). The free energy was approximated by the continuum electrostatic free energy, where the protein and ligand atoms are explicitly included but the solvent is replaced by a dielectric continuum. The free energy change in either medium (protein, solution) can be written as:

$$\Delta G = 1/2\sum_i \delta q_i\left(\langle V_i\rangle_A + \langle V_i\rangle_B\right). \quad (9)$$

The sum is over all the atoms of the titrable group; $\delta q_i$ is the change in the atomic charge due to the protonation; and $V_i$ is the electrostatic potential on atom $i$ when the proton charge is absent. The brackets represent averaging over the ensemble of conformations drawn from an MD simulation when the phosphate is protonated or deprotonated (A and B, respectively; one snapshot every 20 ps over the last 4 ns of MD). The electrostatic potentials were computed for each MD conformation by numerically solving the Poisson–Boltzmann equation of continuum electrostatics, where the protein and ligand were treated as a single dielectric medium with a dielectric constant of 2; solvent was treated as another medium with a dielectric constant of 80, the experimental value for bulk water. A low dielectric value is appropriate for the protein because the conformational changes induced by the proton binding are explicitly modeled (through the use of two MD simulations: one each for the protonated/deprotonated states) [78–80].

The boundary between the two dielectric media was defined as the protein/ligand molecular surface, computed with a 1.6 Å radius probe sphere. For the potential calculation, the system was discretized using a cubic grid with a 68 Å edge and a spacing of 0.4 Å. The Poisson–Boltzmann equation was solved with Coulombic boundary conditions, using the Charmm program (PBEQ module) [91]. We used an ionic strength corresponding to a 0.15 M concentration of monovalent ions, close to the physiological value. The same procedure was followed for GTP in water, using the conformations drawn from the protein simulations. The $Mg^{2+}$ and three waters that coordinate it were treated explicitly, as part of the ligand. The $pK_a$ shift due to the protein environment has the form:

$$pK_{a,prot} - pK_{a,solv} = \frac{\Delta G_{prot} - \Delta G_{solv}}{2.303kT}. \quad (10)$$

### 7.4. Energy calculations for aIF2 with the fixed charge and polarizable force fields

To compare the Charmm27 and AMOEBA force fields, we focus on a quantity $\delta G$ that approximates the free energy to convert GTP into GDP. For a given conformational state, say ON, we consider the solvated protein with bound GTP, and two different charge states for the GTP: the normal charges of GTP (with the particular force field), and a modified set, which mimics the charge distribution in GDP. Specifically, we add a charge of +0.25 to the four terminal atoms of GTP: three oxygens and the phosphorus. We refer to the ligands with the two charge states as L = GTP and L′ = $GTP^0$. The superscript indicates that the terminal phosphate has a reduced charge. The net charge of L is −4; that of L′ is −3. For a given structure, taken from an MD simulation, the energy to change the ligand charge distribution from the L to the L′ values will be denoted $\delta E$. It is analogous to the energy gap for removing an electron instantaneously from a protein structure, which is a standard quantity in electron transfer theory [92]. We will consider an average of $\delta E$ over an ensemble of protein structures, drawn from an MD simulation. We consider two MD simulations, both performed with the Charmm27 force field. The first corresponds to the protein:GTP complex; the second corresponds to a modified, GTP-like ligand, but where the γ-phosphate has its charges set to zero while the β-phosphate charges are those of GDP. These two conformational ensembles, referred to as 1 and 0, are approximately representative of the L and L′ charge states, respectively. Finally, we consider the overall average, $(\langle\Delta E\rangle_1 + \langle\Delta E\rangle_0)/2$, which we denote $\delta G$. Indeed, $\delta G$ represents a linear response approximation to the free energy to transform L into L′. It should be a good indicator of the force field dependency of the MDFE results, and of the additivity hypothesis.

## Acknowledgements

We thank Martin Karplus for the CHARMM program and Elena Zvereva for discussions. Some of the simulations were done at the French national supercomputer center CINES. NAMD was developed by the Theoretical and Computational Biophysics Group in the Beckman Institute at the University of Illinois at Urbana.

## References

[1] S.R. Sprang, G proteins, effectors and GAP's: structure and mechanism, Curr. Opin. Struct. Biol. 7 (1997) 849–856.
[2] I.R. Vetter, A. Wittinghofer, The guanine nucleotide-binding switch in three dimensions, Science 294 (2001) 1299–1304.
[3] M. Perutz, Mechanisms of Cooperativity and Allosteric Regulation in Proteins, Cambridge University Press, Cambridge, 1990.
[4] D.D. Boehr, R. Nussinov, P.E. Wright, The role of conformational ensembles in biomolecular recognition, Nat. Chem. Biol. 5 (2009) 789–796.
[5] B.J. Grant, A.A. Gorfe, J.A. McCammon, Large conformational changes in proteins: signalling and other functions, Curr. Opin. Struct. Biol. 20 (2010) 142–147.
[6] M. Cecchini, A. Houdusse, M. Karplus, Allosteric communication in myosin V: from small conformational changes to large directed movements, PLoS Comput. Biol. 4 (2008) e1000129.
[7] P. Llinas, O. Pylypenko, T. Isabet, Monalisaand Mukherjea, H.L. Sweeney, A.M. Houdusse, How myosin motors power cellular functions: an exciting journey from structure to function, FEBS J. 279 (2012) 551–562.
[8] M.W. Karaman, S. Herrgard, D.K. Treiber, P. Gallant, C.E. Atteridge, B.T. Campbell, K. W. Chan, P. Ciceri, M.I. Davis, P.T. Edeen, R. Faraoni, M. Floyd, J.P. Hunt, D.J. Lockhart, Z.V. Milanov, M.J. Morrison, G. Pallares, H.K. Patel, S. Pritchard, L.M. Wodicka, P.P. Zarrinkar, A quantitative analysis of kinase inhibitor selectivity, Nat. Biotechnol. 26 (2008) 127–132.
[9] L.N. Johnson, Protein kinase inhibitors: contributions from structure to clinical compounds, Q. Rev. Biophys. 42 (2009) 1–40.
[10] V.V. Hauryliuk, GTPases of the prokaryotic translation apparatus, Mol. Biol. 40 (2006) 688–701.
[11] A.G. Myasnikov, A. Simonetti, S. Marzi, B.P. Klaholz, Structure-function insights into prokaryotic and eukaryotic translation initiation, Curr. Opin. Struct. Biol. 19 (2009) 300–309.
[12] M. Karplus, J.A. McCammon, Molecular dynamics simulations of biomolecules, Nat. Struct. Mol. Biol. 9 (2002) 646–651.
[13] T. Simonson, P. Satpati, Simulating GTP:Mg and GDP:Mg with a simple force field: a structural and thermodynamic analysis, J. Comput. Chem. 34 (2013) 836–846.
[14] L. Zheng, M. Chen, W. Yang, Random walk in orthogonal space to achieve efficient free energy simulation of complex systems, Proc. Natl. Acad. Sci. U. S. A. 105 (2008) 20227–20232.
[15] H. Kokubo, T. Tanaka, Y. Okamoto, Two-dimensional replica-exchange method for predicting protein-ligand binding structures, J. Comput. Chem. 34 (2013) 2601–2614.
[16] M. Moradi, E. Tajkhorshid, Computational recipe for efficient description of large-scale conformational changes in biomolecular systems, J. Chem. Theory Comput. 10 (2014) 2866–2880.
[17] S. Park, W. Im, Theory of adaptive optimization for umbrella sampling, J. Chem. Theory Comput. 10 (2014) 2719–2728.
[18] J. Ponder, D.A. Case, Force fields for protein simulations, Adv. Protein Chem. 66 (2003) 27.
[19] A. Warshel, M. Kato, A.V. Pisliakov, Polarizable force fields: history, test cases, and prospects, J. Chem. Theory Comput. 3 (2007) 2034–2045.
[20] G. Hummer, L. Pratt, A. Garcia, B.J. Berne, S.W. Rick, Electrostatic potentials and free energies of solvation of polar and charged molecules, J. Phys. Chem. B 101 (1997) 3017–3020.
[21] Y.L. Lin, A. Aleksandrov, T. Simonson, B. Roux, Electrostatic free energy computations for solutions and proteins, J. Chem. Theory Comput. 10 (2014) 2690–2709.
[22] E. Schmitt, M. Naveau, Y. Mechulam, Eukaryotic and archaeal translation initiation factor 2: a heterotrimeric tRNA carrier, FEBS Lett. 584 (2010) 405–412.

[23] T. Simonson, P. Satpati, Nucleotide recognition by the initiation factor aIF5B: free energy simulations of a neo-classical GTPase, Proteins 80 (2012) 2742–2757.
[24] E. Schmitt, L. Yatime, Y. Mechulam, The large subunit of initiation factor aIF2 is a close structural homologue of elongation factors, EMBO J. 21 (2002) 1821–1832.
[25] P. Satpati, C. Clavaguéra, G. Ohanessian, T. Simonson, Free energy simulations of a GTPase: GTP and GDP binding to archaeal Initiation Factor 2, J. Phys. Chem. B 115 (2011) 6749–6763.
[26] P. Satpati, T. Simonson, Conformational selection through electrostatics: free energy simulations of GTP and GDP binding to archaeal Initiation Factor 2, Proteins 80 (2012) 1264–1282.
[27] P. Satpati, T. Simonson, Conformational selection by the aIF2 GTPase: a molecular dynamics study of functional pathways, Biochemistry 51 (2012) 353–361.
[28] A. Roll-Mecak, C. Cao, T.E. Dever, S.K. Burley, X-ray structures of the universal translation initiation factor IF2/eIF5B: conformational changes on GDP and GTP binding, Cell 103 (2000) 781–792.
[29] B.-S. Shin, D. Maag, A. Roll-Mecak, M.S. Arefin, S.K. Burley, J.R. Lorsch, T.E. Dever, Uncoupling of Initiation Factor eIF5B/IF2 GTPase and translational activities by mutations that lower ribosome affinity, Cell 111 (2002) 1015–1025.
[30] T.V. Pestova, I.B. Lomakin, J.H. Lee, S.K. Choi, T.E. Dever, C.U.T. Hellen, The joining of ribosomal subunits in eukaryotes requires eIF5B, Nature 403 (2000) 332–335.
[31] V. Hauryliuk, V.A. Mitkevich, A. Draycheva, S. Tankov, V. Shyp, A. Ermakov, A.A. Kulikova, A.A. Makarov, M. Ehrenberg, Thermodynamics of GTP and GDP binding to bacterial Initiation Factor 2 suggests two types of structural transitions, J. Mol. Biol. 394 (2009) 621–626.
[32] M. Pavlov, A. Zorzet, D. Andersson, M. Ehrenberg, Activation of initiation factor 2 by ligands and mutations for rapid docking of ribosomal subunits, EMBO J. 30 (2011) 289–301.
[33] J.-C. Liao, S. Sun, D. Chandler, G. Oster, The conformational states of Mg:ATP in water, Eur. Biophys. J. 33 (2004) 29–37.
[34] D. Thompson, T. Simonson, Molecular dynamics simulations show that bound $Mg^{2+}$ contributes to amino acid and aminoacyl adenylate binding specificity in aspartyl-tRNA synthetase through long range electrostatic interactions, J. Biol. Chem. 281 (2006) 23792–23803.
[35] J.L. Leroy, M. Guéron, Demonstration and characterization of two complexes of cobalt(II) to mononucleotides by $^{31}P$ and $^{1}H$ NMR, J. Am. Chem. Soc. 108 (1986) 5753–5759.
[36] K.M. Callahan, N.N. Casillas-Ituarte, M. Roeselova, H.C. Allen, D.J. Tobias, Solvation of magnesium dication: molecular dynamics simulation and vibrational spectroscopic study of magnesium chloride in aqueous solutions, J. Phys. Chem. A 114 (2010) 5141–5148.
[37] R.N. Goldberg, Y.B. Tewari, Thermodynamics of the disproportionation of adenosine 5′-diphosphate to adenosine 5′-triphosphate and adenosine 5′-monophosphate. I. Equilibrium model, Biophys. Chem. 40 (1991) 241–261.
[38] D.J. Klein, P.B. Moore, T.A. Steitz, The contribution of metal ions to the structural stability of the large ribosomal subunit, RNA 10 (2004) 1366–1379.
[39] R.A. Alberty, R.N. Goldberg, Standard thermodynamic formation properties for the adenosine 5′-triphosphate series, Biochemistry 31 (1992) 10610–10615.
[40] A.C. Storer, A. Cornish-Bowden, Concentration of $Mg:ATP^{2-}$ and other ions in solution, Biochem. J. 159 (1976) 1–5.
[41] V.L. Pecoraro, J.D. Hermes, W.W. Cleland, Stability constants of $Mg^{2+}$ and $Cd^{2+}$ complexes of adenine nucleotides and thionucleotides and rate constants for formation and dissociation of MgATP and MgADP, Biochemistry 23 (1984) 5262–5271.
[42] R.K. Gupta, P. Gupta, W.D. Yushok, Z.B. Rose, Measurement of the dissociation constant of Mg-ATP at physiological nucleotide levels by a combination of $^{31}P$ NMR and optical absorbance spectroscopy, Biochem. Biophys. Res. Commun. 117 (1983) 210–216.
[43] J.W. Ponder, C.J. Wu, P.Y. Ren, V.S. Pande, J.D. Chodera, M.J. Schnieders, I. Haque, D.L. Mobley, D.S. Lambrecht, R.A. DiStasio, M. Head-Gordon, G. Clark, M.E. Johnson, T. Head-Gordon, The current status of the AMOEBA polarizable force field, J. Phys. Chem. B 114 (2010) 2549–2564.
[44] Jay Ponder Lab, TINKER Software Tools for Molecular Design, Department of Biochemistry and Molecular Biophysics, Washington University School of Medicine, Saint Louis, U.S.A., 1987–2011
[45] T. Simonson, Free energy calculations, in: O. Becker, A. Mackerell Jr., B. Roux, M. Watanabe (Eds.), Computational Biochemistry & Biophysics, Marcel Dekker, N.Y., 2001, (ch. 9).
[46] C. Chipot, A. Pohorille, Free energy Calculations: Theory and Applications in Chemistry and Biology, Springer Verlag, N.Y., 2007
[47] S. De Leeuw, J. Perram, E. Smith, Simulation of electric systems in periodic boundary conditions. I. Lattice sums and dielectric constants, Proc. Roy. Soc. London A373 (1980) 27–56.
[48] B.R.A. Nijboer, T.W. Ruijgrok, On the energy per particle in three- and two-dimensional Wigner lattices, J. Stat. Phys. 53 (1988) 361–382.
[49] F.E. Figueirido, R. Levy, On finite-size effects in computer simulations using the Ewald potential, J. Chem. Phys. 103 (1995) 6133–6142.
[50] T. Darden, Treatment of long-range forces and potential, in: O. Becker, A. Mackerell Jr., B. Roux, M. Watanabe (Eds.), Computational Biochemistry & Biophysics, Marcel Dekker, N.Y., 2001, (ch. 4).
[51] J. Barker, R. Watts, Monte Carlo studies of the dielectric proterties of water-like models, Mol. Phys. 26 (1973) 789–792.
[52] W. van Gunsteren, H. Berendsen, J. Rullmann, Inclusion of reaction fields in molecular dynamics: application to liquid water, Faraday Discuss. Chem. Soc. 66 (1979) 58–70.
[53] E. Harder, B. Roux, On the origin of the electrostatic potential difference at a liquid-vacuum interface, J. Chem. Phys. 129 (2008) 234706.
[54] R. Godement, Analyse Mathématique I, Springer, Berlin, 1998.
[55] G. Hummer, L. Pratt, A. Garcia, S. Garde, B.J. Berne, S.W. Rick, Reply to comment on "electrostatic potentials and free energies of solvation of polar and charged molecules", J. Phys. Chem. B 102 (1998) 3841–3843.
[56] T. Darden, D. Pearlman, L. Pedersen, Ionic charging free energies: spherical versus periodic boundary conditions, J. Chem. Phys. 109 (1998) 10921–10935.
[57] J. Aqvist, T. Hansson, On the validity of electrostatic linear response in polar solvents, J. Phys. Chem. 100 (1996) 9512–9521.
[58] A.D. Mackerell, D. Bashford, M. Bellott, R.L. Dunbrack, J. Evanseck, M.J. Field, S. Fischer, J. Gao, H. Guo, S. Ha, D. Joseph, L. Kuchnir, K. Kuczera, F.T.K. Lau, C. Mattos, S. Michnick, T. Ngo, D.T. Nguyen, B. Prodhom, W.E. Reiher, B. Roux, J. Smith, R. Stote, J. Straub, M. Watanabe, J. Wiorkiewicz-Kuczera, D. Yin, M. Karplus, An all-atom empirical potential for molecular modelling and dynamics study of proteins, J. Phys. Chem. B 102 (1998) 3586–3616.
[59] T. Simonson, G. Archontis, M. Karplus, Continuum treatment of long-range interactions in free energy calculations. Application to protein-ligand binding, J. Phys. Chem. B 101 (1997) 8349–8362.
[60] T. Simonson, Electrostatic free energy calculations for macromolecules: a hybrid molecular dynamics/continuum electrostatics approach, J. Phys. Chem. B 104 (2000) 6509–6513.
[61] W. Im, S. Bernèche, B. Roux, Generalized solvent boundary potential for computer simulations, J. Chem. Phys. 114 (2001) 2924–2937.
[62] X. Lu, Q. Cui, Charging free energy calculations using the Generalized Solvent Boundary Potential (GSBP) and periodic boundary condition: a comparative analysis using ion solvation and oxidation free energy in proteins, J. Phys. Chem. B 117 (2012) 2005–2018.
[63] V. Hauryliuk, S. Hansson, M. Ehrenberg, Cofactor dependent conformational switching of GTPases, Biophys. J. 95 (2008) 1704–1715.
[64] J. McCammon, Theory of biomolecular recognition, Curr. Opin. Struct. Biol. 8 (1998) 245–249.
[65] T. Simonson, G. Archontis, M. Karplus, Free energy simulations come of age: the protein–ligand recognition problem, Acc. Chem. Res. 35 (2002) 430–437.
[66] W.L. Jorgensen, The many roles of computation in drug discovery, Science 303 (2003) 1813–1818.
[67] C. Chipot, A.E. Mark, V.S. Pande, T. Simonson, Significant applications of free energy calculations to chemistry and biology, in: C. Chipot, A. Pohorille (Eds.), Free Energy Calculations: Theory and Applications in Chemistry and Biology, Springer Verlag, N. Y., 2007, (ch. 13).
[68] A. Aleksandrov, D. Thompson, T. Simonson, Alchemical free energy simulations for biological complexes: powerful but temperamental…, J. Mol. Recognit. 23 (2010) 117–127.
[69] B. Tembe, J.A. McCammon, Ligand-receptor interactions, Comput. Chem. 8 (1984) 281–283.
[70] W. Yang, Y.Q. Gao, Q. Cui, J. Ma, M. Karplus, The missing link between thermodynamics and structure in F1-ATPase, Proc. Natl. Acad. Sci. U. S. A. 100 (2003) 874–879.
[71] Y.Q. Gao, W. Yang, M. Karplus, A structure-based model for the synthesis and hydrolysis of ATP by F1-ATPase, Cell 123 (2005) 195–205.
[72] L. Yatime, Y. Mechulam, S. Blanquet, E. Schmitt, Structural switch of the γ subunit in an archaeal aIF2 α γ heterodimer, Structure 14 (2006) 119–128.
[73] L. Yatime, Y. Méchulam, S. Blanquet, E. Schmitt, Structure of an archaeal heterotrimeric initiation factor 2 reveals a nucleotide state between the GTP and the GDP states, Proc. Natl. Acad. Sci. U. S. A. 104 (2007) 18445–18450.
[74] R.M. Voorhees, T.M. Schmeing, A.C. Kelley, V. Ramakrishnan, The mechanism for activation of GTP hydrolysis on the ribosome, Science 330 (2010) 835–838.
[75] D.C. Bas, D.M. Rogers, J.H. Jensen, Very fast prediction and rationalization of $pK_a$ values for protein–ligand complexes, Proteins (2008) 765–783.
[76] M.H.M. Olsson, C.R. Sondergaard, M. Rostowski, J.H. Jensen, PROPKA3: consistent treatment of internal and surface residues in empirical $pK_a$ predictions, J. Chem. Theory Comput. 7 (2011) 525–537.
[77] T. Simonson, J. Carlsson, D.A. Case, Proton binding to proteins: $pK_a$ calculations with explicit and implicit solvent models, J. Am. Chem. Soc. 126 (2004) 4167–4180.
[78] Y. Sham, Z. Chu, A. Warshel, Consistent calculations of $pK_a$'s of ionizable residues in proteins: semi-microscopic and microscopic approaches, J. Phys. Chem. B 101 (1997) 4458–4472.
[79] I. Eberini, A. Baptista, E. Gianazza, F. Fraternali, T. Beringhelli, Reorganization in apo- and holo-β-lactoglobulin upon protonation of Glu89: molecular dynamics and $pK_a$ calculations, Proteins 54 (2004) 744–758.
[80] G. Archontis, T. Simonson, Proton binding to proteins: a free energy component analysis using a dielectric continuum model, Biophys. J. 88 (2005) 3888–3904.
[81] A. Aleksandrov, J. Proft, W. Hinrichs, T. Simonson, Protonation patterns in tetracycline:Tet repressor recognition: Simulations and experiments, ChemBioChem 8 (2007) 675–685.
[82] T. Simonson, Protein:ligand recognition: simple models for electrostatic effects, Curr. Pharm. Des. 19 (2013) 4241–4256.
[83] C.N. Pace, G.R. Grimsley, J.M. Scholtz, Protein ionizable groups: $pK_a$ values and their contribution to protein stability and solubility, J. Biol. Chem. 284 (2009) 13285–13289.
[84] Y. Shi, Z. Xia, J. Zhang, R. Best, C. Wu, J.W. Ponder, P.Y. Ren, Polarizable atomic multipole-based AMOEBA force fieldfor proteins, J. Chem. Theory Comput. 9 (2013) 4046–4064.
[85] P.E.M. Lopes, J. Huang, J. Shim, Y. Luo, H. Li, B. Roux, A.D. MacKerell Jr., Polarizable force field for peptides and proteins based on the classical Drude oscillator, J. Chem. Theory Comput. 9 (2013) 5430–5449.
[86] N. Foloppe, A.D. MacKerell Jr., All-atom empirical force field for nucleic acids: I. Parameter optimization based on small molecule and condensed phase macromolecular target data, J. Comput. Chem. 21 (2000) 86–104.

[87] W. Jorgensen, J. Chandrasekar, J. Madura, R. Impey, M. Klein, Comparison of simple potential functions for simulating liquid water, J. Chem. Phys. 79 (1983) 926–935.
[88] B. Brooks, C.L. Brooks III, A.D. Mackerell Jr., L. Nilsson, R.J. Petrella, B. Roux, Y. Won, G. Archontis, C. Bartels, S. Boresch, A. Caflisch, L. Caves, Q. Cui, A.R. Dinner, M. Feig, S. Fischer, J. Gao, M. Hodoscek, W. Im, K. Kuczera, T. Lazaridis, J. Ma, V. Ovchinnikov, E. Paci, R.W. Pastor, C.B. Post, J.Z. Pu, M. Schaefer, B. Tidor, R.M. Venable, H.L. Woodcock, X. Wu, W. Yang, D.M. York, M. Karplus, CHARMM: the biomolecular simulation program, J. Comput. Chem. 30 (2009) 1545–1614.
[89] J.C. Phillips, R. Braun, W. Wang, J. Gumbart, E. Tajkhorshid, E. Villa, C. Chipot, R.D. Skeel, L. Kale, K. Schulten, Scalable molecular dynamics with NAMD, J. Comput. Chem. 26 (2005) 1781–1802.
[90] P.A. Kollman, Free energy calculations: applications to chemical and biochemical phenomena, Chem. Rev. 93 (1993) 2395.
[91] W. Im, D. Beglov, B. Roux, Continuum solvation model: computation of electrostatic forces from numerical solutions to the Poisson–Boltzmann equation, Comput. Phys. Commun. 111 (1998) 59–75.
[92] T. Simonson, Electrostatics and dynamics of proteins, Rep. Prog. Phys. 66 (2003) 737–787.